Aftershock Analysis for the 1997 Ghaen-Birjand (Ardekul) Earthquake

Amir Mansour Farahbod[1], Conrad Lindholm[2], Mohammad Mokhtari[3], and Hilmar Bungum[4]

1. Research Associate, Seismology Research Centre, International Institute of Earthquake Engineering and Seismology (IIEES), I.R. Iran, email: Farahbod@ dena.iiees.ac.ir
2. Associate Professor, Seismology Department of NORSAR, Norway, email: Conrad@norsar.no
3. Associate Professor, Director of IIEES Seismology Research Centre, email: Mokhtari@dena.iiees.ac.ir
4. Senior Seismologist, Head of NORSAR Seismology Department, Norway, email: Hilmar@norsar.no

ABSTRACT: *In this study at the first step, the database of two temporary networks of International Institute of Earthquake Engineering and Seismology (IIEES) and Institute of Geophysics of Tehran University (IGTU), which deployed independently after the Ghaen-Birjand earthquake, were merged. Based on the new database, focal mechanisms of some larger aftershocks were obtained and crustal model of eastern Iran [3] modified for the epicentral area of Ghaen-Birjand earthquake and its aftershocks. The Vp/Vs ratio is inferred as 1.85 for the region covered by the temporary seismic networks. After relocation of more than two hundred events, it was cleared that at least three of the largest aftershocks were estimated to be located with a precision corresponding to error ellipsoid axes within 5 to 10 km (Ground Truth level of 5 to 10).*

Keywords: Aftershock; Ghaen-Birjand; Velocity model; Focal mechanism

1. Introduction

On May 10, 1997 at 12:27 (local time), an earthquake with magnitude *Mw* 7.3 (*USGS*), 7.2 (Harvard), *Me* 7.7 (*USGS*), *Ms* 7.2 (Berkeley) occurred in the Ghaen-Birjand region in northeastern Iran. The radiated energy and seismic moment of this event estimated to be $Es = 8.9 \times 10^{15}$ *Nm* (*USGS*), $Mo = 9.5 \times 10^{19}$ *Nm* (*USGS*), $Mo = 7.3 \times 10^{19}$ *Nm* (Harvard) respectively. The earthquake was felt over a large area including the cities of Mashad, Kerman and Yazd. The epicenter of the earthquake was located close to the town village of Ardekul at 33.88°*N* latitude and 59.82°*E* longitude according to *ISC* report. Most of the damage and human casualty occurred in a 100*km* strip between Birjand and Ghaen.

The epicenter of Ghaen-Birjand earthquake is situated in the north of Sistan collision zone which separates the central Iranian block on the west from the Afghan block on the east [17, 6]. This region is well known for destructive earthquakes. The last large earthquakes in this region were occurred in 1979. One was the Korizan earthquake with magnitude *Ms* 6.6 on November 14, 1979 and another was the Koli-Boniabad earthquake with magnitude *Ms* 7.1 on November 27, 1979 [1]. The Korizan earthquake occurred in the same area and along the northern part of the same fault (Korizan fault) associated with this most recent event, see Figure (1).

As a result of the recent earthquake, 1,567 people were killed, and more than 2,300 were injured. In addition, 147 villages experienced damage. Some of these villages were completely destroyed while many others suffered heavy damage, especially to housing units. From the observed damage, an intensity of *X* on
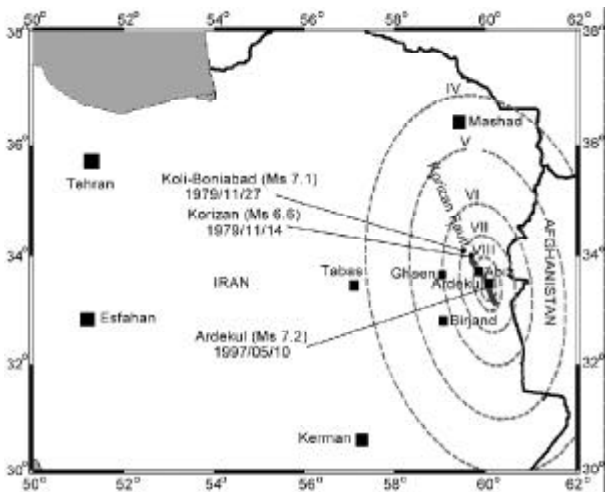
Figure 1. Isoseismic map of the Ghaen-Birjand earthquake area, Korizan fault and the largest events near the fault during the past two decades. This map was originally taken from Michael West, Columbia University (1999), with some modifications.

the *MSK* scale was assigned to affected areas in the close vicinity of the epicenter. The peak ground acceleration (*PGA*) at places close to the epicenter is estimated to have been about 0.7*g* [13].

This event followed by a large number of after-shocks as large as Ms 5.9.

In the present paper some of the recorded aftershocks and the results derived from their analysis will be discussed.

2. The Database

Shortly after this event, both *IGTU* and *IIEES* installed temporary networks in the epicentral area [15, 14]. The temporary network of *IIEES* consisted of five stations with an operating period of approximately 7 weeks, starting May 13, 1997. *IGTU* deployed a temporary network of 15 stations 5 days after the main shock which operated for a period of two months, and in November 1997 *IGTU* installed a small local network of five stations near the southern end of the fault, aimed for monitoring the aftershock activity and their possible migration. This network was in operation for one month. Recorders, which were deployed by *IIEES*, were Kinemetrics *SSR1* with *SS*-1 seismometers while *IGTU* used three *MEQ*-800 analogue recorders and twelve *PDAS*-100. All the recorders used radio signals via *WWVT* receivers for time setting.

The first step in the present analysis was merging the two datasets and establishing a joint database for the time period in which a maximum coverage existed. This resulted in a database of 215 aftershocks

recorded over a period of 48 days from May 15 until July 1. As the main goal of this paper is improving the location of the aftershocks, the new database was consisted of the events, which were recorded by the both networks.

Time distribution of recorded aftershocks in the new database is shown in Figure (2). The distribution in Figure (2) is regarded as quite normal for an aftershock sequence following such a large earth-quake.

The modified Omori relation could characterize the rate of aftershock decay for this event as Eq. (1) [7]:

$$N(t) = 246.4t^{-0.63} \tag{1}$$

In which $N(t)$ denotes the number of aftershocks, t days after the main shock. It must be noted that Figure (2) only shows the number of events recorded by the both networks and it does not indicate the seismic activity. On day 26 due to some instrumental problems, no common event was recorded by the networks.
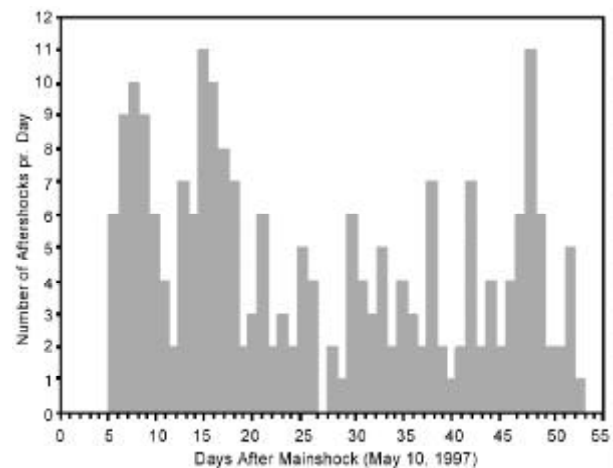

Figure 2. Number of events per day in the aftershock sequence of the 1997 Ghaen-Birjand earthquake which was recorded by the both networks, from five days after the main shock, covering about two months of recording.

3. *Vp/Vs* Ratio

Estimation of Vp/Vs ratios is useful to examine the accuracy of the readings of *S* arrival times in the regions where this ratio was previously obtained. *S* waves are in some cases very difficult to interpret on seismograms.

The *Vp/Vs* ratio was estimated for the aftershocks of Ghaen-Birjand earthquake, recorded by local temporary networks. Figure (3a) shows the fitting

of regression line in the relation between P and *S-P* times. The *Vp/Vs* ratio and its standard deviation for 262 couples of *P* and *S-P* times among 215 events are 1.853 and 0.033 respectively. In this way all the low quality data that the standard deviation of the residual of *P* times are beyond 0.5 second, were excluded. Also Wadati diagram for the aftershock events is shown in Figure (3b). The maximum number of occurrence can be observed between 1.82 to 1.87 for *Vp/Vs*. Berberian [4] studied the aftershocks of the 1978 Tabas-e-Golshan earthquake in eastern Iran (approximately 200*km* west of the city of Ghaen) and obtained the same value of 1.85 for the *Vp/Vs* ratio.

Figure 4. The epicentre distribution of the aftershocks following the Ghaen-Birjand 1997 earthquake after relocation with improved model, and plotted together with the fault surface trace and focal mechanisms (Harvard CMT) from the main event and the largest aftershock. The temporary stations (both IGTU and IIEES) are shown with black triangles.
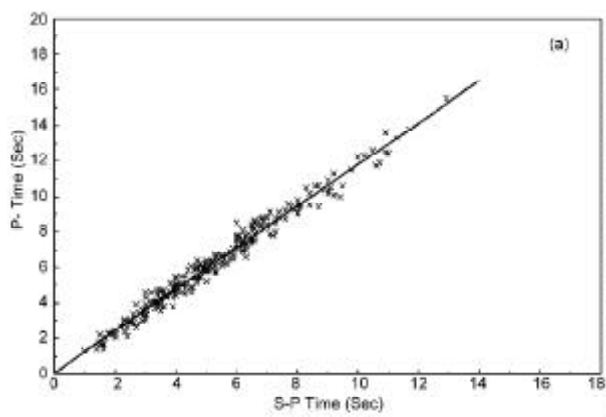

Figure 3a. P time versus S-P time for the aftershocks of the 1997 Ghaen-Birjand earthquake based on the data that recorded by both two temporary networks.
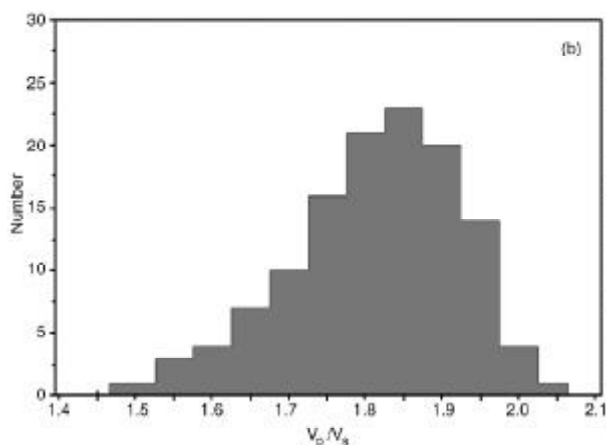

Figure 3b. Wadati diagram for the aftershocks.

4. Crustal Model and Focal Mechanisms

The epicenter location of the main shock, reported by ISC and the relocated aftershocks of Ghaen-Birjand earthquake are shown in Figure (4). These locations were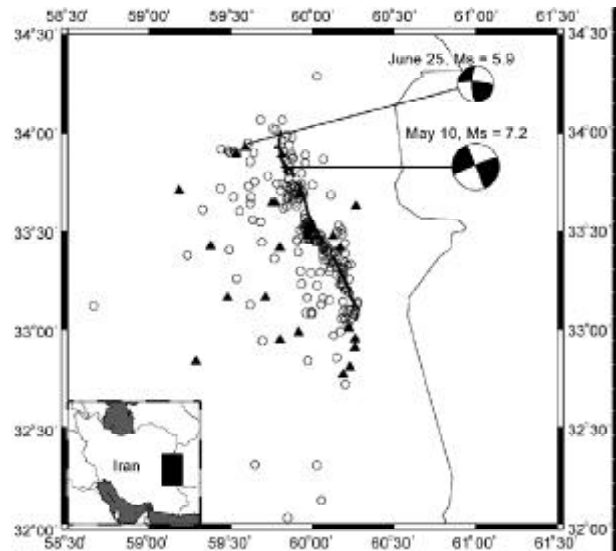 obtained based on a 1-*D* inversion using the *VELEST* algorithm of Kissling [9, 10, 11]. Before running the *VELEST* program, 33 well-located aftershocks were selected in which the *RMS*< 0.2, number of phases > 8 and the absolute location error is less than 5*km*. In this case, the event locations are relatively stable and it is possible to estimate reasonable velocity models by using the method of minimizing average *RMS*.

The program *VELEST* is used to solve the coupled hypocenter velocity model problem for local earthquakes. It performs a simultaneous inversion for hypocenters and velocity model. The inversion is limited to first arriving phases. Based on an initial crustal model, this algorithm uses the arrival times of the aftershock sequence to develop a refined model with simultaneous relocation of the events.

As an initial value, the modified Tabas velocity model [2, 3] for eastern Iran was used. The *P* velocity in the first layer of starting model is 5.7*km/s* and its thickness is 15*km* which overlies a lower crust with *Vp* = 6.10*km/s*. The last layer has a *Vp* =7.70*km/s*, see Table (1). For this model the average *RMS* is 0.179s for 33 aftershocks. The results of minimizing average *RMS* are *Vp* = 5.73*km/s* in the first layer with 13*km* thickness and *Vp* = 6.03*km/s* in the second layer with 9*km* thickness. Trying to minimize the *RMS*, a new layer was introduced beneath the second layer in which the best parameters were estimated as

Table 1. Initial model for eastern Iran [3] and improved model based on inversion process of Ghaen-Birjand after shocks. RMS indicates average root-mean-square values of the travel time residuals for both initial and improved models for all the aftershocks.

Parameters	Layer	V_p (km/s)	V_s (km/s)	D (km)
Bahavar Model [3] for eastern Iran	1	5.70	3.08	0.0
	2	6.10	3.29	15.0
	3	7.70	4.16	43.0
Average RMS (s) for 33 well-located events	0.179			
Improved Model for eastern Iran (After inversion)	1	5.71	3.08	0.0
	2	5.96	3.22	12.0
	3	6.53	3.52	23.0
	4	7.70	4.16	43.0
Average RMS (s) for 33 well-located events	0.127			

Figure 5. Depth distribution (in kilometers) of the aftershocks in Ghaen-Birjand area in a NE-SW cross-section. The line in the bottom of aftershocks shows the Moho discontinuity at the depth of 43 kilometers.

$Vp = 6.55km/s$ and $10km$ thickness. Due to short site-source distances within the local network, the velocity of the last layer and Moho depth were assigned as a fixed value. For this model, the average *RMS* for 33 well-located aftershocks is $0.133s$. To verify these results, by using the *VELEST* program, a 1-*D* inversion of arrival times for the same events has been carried out. Using the results of minimizing average method, 1-*D* inversion converged to the final model, which is in good agreement with the results of the last step, see Table (1). The proposed crustal model for the Ghaen-Birjand area reduces the average *RMS* for locating the whole events in the database (215 aftershocks) from 0.381 for the model of eastern Iran [3] to 0.329.

Based on the improved model, the aftershocks were relocated and plotted in Figure (4). In addition to epicentre distributions, the stations of temporary networks, fault trace (with a length about $110km$) and the Harvard moment tensor (focal mechanism) solutions for the main shock and the largest aftershock are also shown in Figure (4). Focal depth distribution of the aftershocks in a Northeast-Southwest cross-section is given in Figure (5). The aftershock database as displaced in Figures (4) and (5), show some characteristic features:

❖ The epicentres closely follow the main trace, however, with significant activity to the west within the network. This distribution clearly reflects the location of the temporal networks, but also shows that a very large volume around the causative fault experienced aftershock activity.
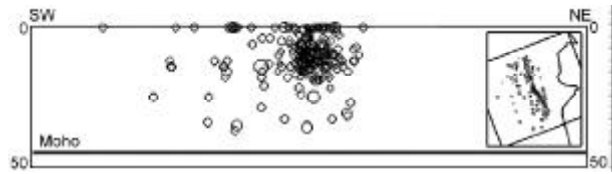
❖ The aftershocks that occurred close to the fault trace shows concentration in two pockets of enhanced seismicity but the largest aftershocks occurred near the northern end of causative fault.

❖ The depth profile in Figure (5) shows that the aftershock activity was concentrated in the upper $25km$ of the crust with a median value about $11km$. Also this figure clarifies a nearly vertical trend, which is in agreement with the main shock faulting.

Most of the westward scatter in Figure (4) is considered to be real, including also the location of the largest aftershock (June 25, 1997, *Ms* 5.9), which could be correlated with a surface rupture.

Eastern Iran is a wide zone of active deformation related to the collision between the Arabian Plate and the Eurasian Plate. The overall shear across the zone is accommodated on both strike-slip and thrust faults in complex geometries. The major earthquakes in the northeast of Iran are associated with *E-W* running thrust and left-lateral strike-slip faults. To the south of these faults is a set of right-lateral strike-slip faults running *N-S* and extending to the Makran region in the south. Seismicity decreases dramatically east of the Iran-Afghanistan border, and geological structures in eastern Iran are aligned in a *N-S* direction. The combination of the dominant *E-W* left-lateral faults and the subordinate *N-S* right-lateral strike-slip faults with thrust faults trending *NW-SE* indicates that the eastern part of the Iranian plateau is undergoing a structural rotation as it is being compressed against the stable blocks of western Afghanistan and Turkmenistan. The rotation results in a lateral movement of material away from the compression zone and towards the Makran region in the south along the strike-slip faults [8].

For earthquakes of the size like the Ghaen-Birjand, the focal mechanisms are often very complicated and the results derived from far field stations were used to interpret the rupture procedure. The source

mechanism of the main shock proposed by Harvard University indicates a right-lateral fault. This agrees with field results of the active fault survey teams.

Based on *P* wave first motion polarity, recorded at local and regional stations, an attempt has been made for calculating fault plane solution of some larger aftershocks. The results of this procedure are presented in Table (2) and from these it can be observed that some of the fault planes exhibit nodal planes that strike in a *N-NW* to *S-SE* direction, in accordance with the main fault and the general geological structural trend. The obtained focal mechanisms do however clearly demonstrate that the aftershock sequence is complicated, and do not adjust on a well-defined rupture plane.

5. Errors in Location

The location errors of aftershocks in latitude, longitude and depth are displayed in Figure (6), with a dashed line drawn at the important *GT5* level
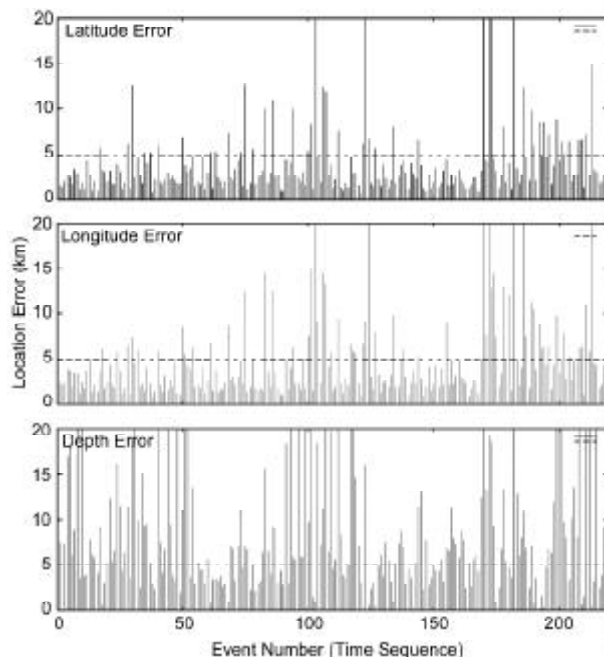

Figure 6. Location errors in latitude, longitude and depth (in km) for the Ghaen-Birjand 1997 aftershock sequence, after relocation with improved crustal model following the VELEST inversion.

Table 2. Fault plane solutions of some larger aftershocks based on P-wave first motion analysis, recorded at local and regional stations. In this table SK, DA, SA, AZ and PL are abbreviations for strike, dip angle, slip angle, azimuth and plunge respectively.

Event (Location)	SK1	DA1	SA1	SK2	DA2	SA2	P-axis AZ	P-axis PL	T-axis AZ	T-axis PL	N-axis AZ	N-axis PL	Projection
1997/06/20 00:32:57.7 Lat: 33.85N Long: 59.95E Depth: 10 ML: 3.2	240	77	-121	129	33	-24	117	49	354	26	248	30	
1997/06/20 12:57:49.2 Lat: 33.29N Long: 60.11E Depth: 25 ML: 4.9	226	58	-160	125	73	-33	82	35	179	10	282	53	
1997/06/21 08:45:26.9 Lat: 33.30N Long: 60.01E Depth: 12 ML: 4.2	40	65	156	299	68	27	350	2	259	34	84	56	
1997/06/22 22:52:57.8 Lat: 33.46N Long: 59.65E Depth: 16 ML: 4.3	271	54	29	163	67	140	220	8	122	44	318	45	
1997/06/23 22:23:18.8 Lat: 33.50N Long: 59.98E Depth: 13 ML: 4.0	44	84	175	134	85	6	269	1	359	8	170	82	

(hypocenter uncertainty less than or equal to 5*km*). Since it is well known that small standard errors can also be caused by using small number of stations (and readings) and thereby not expressing the real precision, in Figure (7) the situation for the present database was clarified. The left part of Figure (7) shows that *RMS* could be controlled by using 6 to 10 stations generally in use (with both *P* and *S* readings from each one). Figure (7 right) shows the *RMS* time residual distribution indicating satisfactory values. It must be noted that the events with *RMS* above 0.6 were excluded from the database of aftershocks.

The three selected aftershocks that were recorded both on local and regional stations relocated using only the data from temporal networks. A main source of uncertainty in the relocation was the focal depth. In this area the depth of earthquakes are generally less than 30*km* and most probably between 9 to 15*km* for the recent events [5]. Based on spectral analysis of 24 Ghaen-Birjand aftershocks with magnitude above 3.0, it has been observed that the most energetic events occurred in northern parts of the fault (near the main shock) and the depth of these events is less than 30*km* [7].
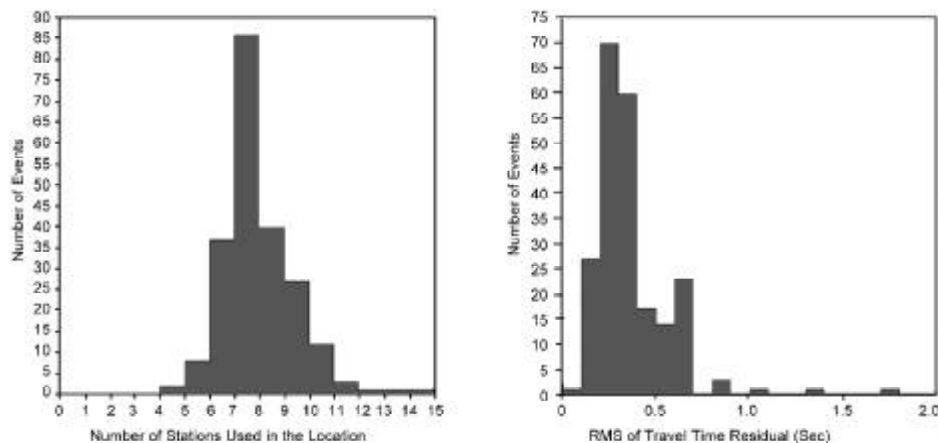

Figure 7. Number of stations used and RMS of travel time residuals for the Ghaen-Birjand 1997 aftershock sequence, after relocation with improved crustal model.

Low *RMS* alone does not, as already noted, guarantee a reliable solution. However, the low average values indicate that station timing for the two networks involved is reliable.

It is notable that the magnitudes for most of the better located aftershocks are too small to be useful as ground truth (*GT*) or reference events, since they should not be expected to record at sufficiently enough stations at regional distances. In order to face this challenge, three of the larger aftershocks listed in Table (3) as candidates.

For the event of May 10, 1997 (main shock) the determined depth by *ISC* was 6.7*km* based on routine inversion methods and *pP_Depth* was 20.25*km*. The *ISC* reports of focal depth for the three aftershocks are as follows:

❖   1997/06/21, Depth 23.3*km*.
❖   1997/06/22, Depth 43.2*km* (*pP_Depth*: 16.06).
❖   1997/06/25, Depth 35.0*km* (*pP_Depth*: 14.27).

In the routine location procedures, the error ellipsoid is computed from the partial derivatives of travel times with respect to latitude, longitude and

Table 3. Three of the Ghaen-Birjand 1997 relocated aftershocks, with time, location (with uncertainties), RMS, different magnitudes and number of stations contribute to ISC solutions.

Date	Time	Lat. N	Long. E	Depth Km	No. P&S	RMS Sec	M_L	Mb	Ms	Mw HRV	No. ISC
1997/06/21	08:45:26.9	33.299	60.008	12	14	0.79	4.2	4.2	3.7	-	48
Error (km)		*5*	*10*	*0*							
1997/06/22	22:52:57.8	33.461	59.651	16	18	0.48	4.3	4.3	3.9	-	73
Error (km)		*1*	*3*	*0*							
1997/06/25	19:38:42.8	33.946	59.606	14	21	0.48	5.3	5.4	5.9	6.0	541
Error (km)		*2*	*3*	*0*							

depth, evaluated at the final hypocenter determined for the earthquake. The travel times are not linear. Consequently, the error ellipsoid is an appropriate measure of the errors only to the extent that the partial derivatives are linear in the region nearby the final location and that there is only one spatial minimum of *RMS* residual. But often there is a minimum in *RMS* residual at two different depths, and sometimes neither minimum is significantly lower than the other.

For the aftershock of June 21 it was difficult to determine focal depth reliably only from the first arrivals. The station *HAJ* recorded the event at 26*km* epicentral distance, and the record shows two secondary phases arriving 2.2 and 3.3 seconds after the first *P* arrival, see Figure (8). The first of these match a reflection from the 23*km* crustal interface if the focal depth was around 12*km*, while the second
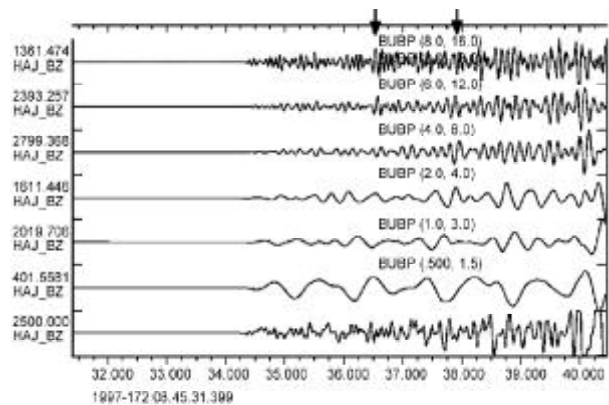

Figure 8. Recording from the HAJ station indicating the secondary arrivals.

phase match a Moho reflection if the focal depth was around 34 km as shown in Figure (9). This figure shows the predicted and observed relative arrival time and the corresponding focal depths. It is seen that the secondary arrivals match with two modelled focal depths of around 12 and around 35*km*. Considering the tectonics of the region and the focal depth of the other aftershocks we are confident that the real focal depth is around 12*km* and it is fixed to that depth in the database. For the second and third events the depths were fixed to calculated *pP* depth. The resulting locations were based on these fixed depth values, which is shown in Table (3).

Table (3) shows the parameters of three aftershocks of Ghaen-Birjand earthquake, which is assigned as potential *GT*5 to *GT*10 candidates with date, time of day, latitude, longitude, depth, No. of *P*
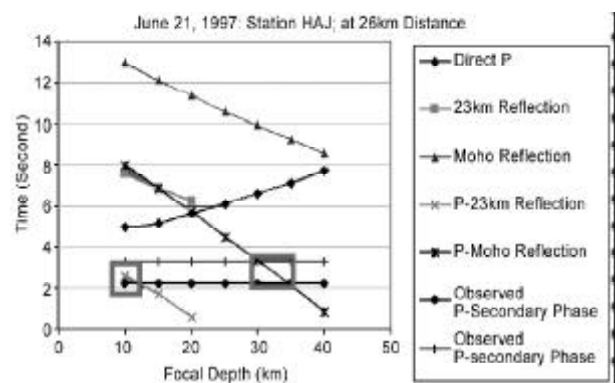

Figure 9. Modelled and observed relative arrival times used for the determination of focal depth for the June 21, 1997, Ghaen-Birjand aftershock. The boxed areas indicate where the possible focal depths match with observed secondary phases.

and *S* phase-readings (No. *P* and *S*), time residual *RMS*, local magnitude *ML*, *mb* (*ISC*), *MS* (*ISC*) and *MW* (*HRV*). The local magnitude (*ML*) calculated according to Eq. (2) which was developed by Farahbod et al [7]:

$$ML = 2.2 log (F\text{-}P) + 0.0002 \boldsymbol{D} \text{-}0.38 \qquad (2)$$

In which *F-P* (*P* time to Final time) is given in seconds and $\boldsymbol{D}$ is epicentral distance in *km*.

In Table (3), standard error estimates in latitude, longitude and depth, in *km*, are given below each of the corresponding values in italics. "No. *ISC*" indicates number of stations that contribute to the *ISC* solutions. The key parameters in consideration of the events in Table (3) as *GT*5 to *GT*10 candidates are the standard errors, indicating that the last two of these, seem to have the best locations. With a magnitude of *Ms* 5.9 which recorded on 541 stations worldwide, the largest aftershock is clearly also large enough in magnitude to serve as a *GT* event.

6. Origin Time Uncertainty for Ghaen-Birjand Aftershocks

The three Ghaen-Birjand aftershocks were located using data (readings) from integrated local networks. The epicentral distances vary from 4*km* up to 120*km* for the local stations, and the azimuths have an acceptable but not very good coverage as shown in Figure (10). With the given distance distribution, the main contributor to the origin time uncertainty is the local velocity model used.

To investigate the effect of the velocity model on the origin time, the three events were located with two alternative velocity models for Iran, Moazami-Goudarzi [12] and Sweeney and Walter [16]).
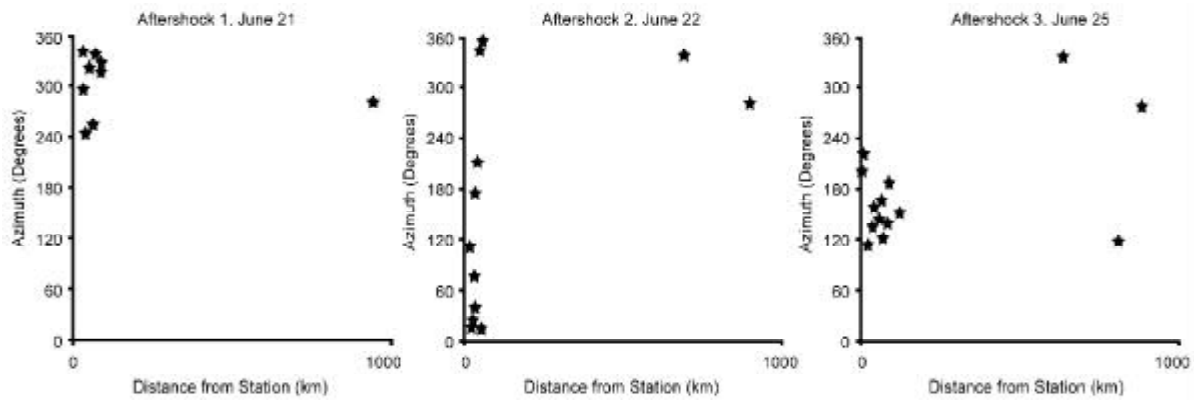
Figure 10. Distance-azimuth distribution for the three Ghaen-Birjand aftershocks. Note that only the stations in the temporary networks were used in the location.

The impacts of the different models are estimated and the maximum differences between origin times assigned as time uncertainty as shown in Table (4).

Table 4. Estimated origin time uncertainty for the three Ghaen-Birjand aftershocks.

Event	Origin Time	Estimated Origin Time Uncertainty
Aftershock 1, June 21	08:45:26.87	0.18 (sec)
Aftershock 2, June 22	22:52:57.85	0.74 (Sec)
Aftershock 3, June 25	19:38:42.75	0.40 (Sec)

7. Summary and Conclusions

Following the May 10, 1997, Ghaen-Birjand earth-quake, two independent temporal networks acquired data from aftershocks for a period of about 2 months. The data from these networks were successfully merged, and 215 aftershocks that were recorded on both networks in the local magnitude range of 2.5 to 5.3 were located in and around the larger rupture zone. The aftershocks spanned in an area of around 100*km* length and 30*km* width.

The aftershocks that occurred close to the fault trace show concentration in two "pockets" of enhanced seismicity, and in general the aftershock activity is more pronounced in the southern end of the ruptured fault. The largest earthquakes occurred near the northern end of the ruptured fault.

Based on this aftershock database a *Vp/Vs* ratio of 1.85 was confirmed for the region, and based on studies from adjacent regions [4] we have substantiated that this value may be representative for the crust in eastern Iran.

A new velocity model was established through joint inversion for hypocenters and crustal velocity structure. The inversion was based on a high quality subset of the database and led to an overall improvement in average *RMS* of travel time residual as compared with the original crustal model.

The proposed crustal model for the Ghaen-Birjand area reduces the average *RMS* for locating the whole events in the database (215 aftershocks) from 0.381 for the model of eastern Iran [3] to 0.329. Based on the following reasons, this new model is a preferred one for the eastern Iran:

1. It improved the initial model for eastern Iran by changing the body wave velocities and the thickness of layers. In the old model, surface wave dispersion data were used for determining the thickness of each layer, Moho depth and velocities. Therefore, by using the data of body waves in local distances through minimizing the average *RMS* and *VELEST* algorithm of Kissling [9] better values for velocity and thickness of each layer in the upper crust were obtained.

2. The extent of aftershock distribution is about 100*km* in length and 30*km* in width, so the obtained model is not constrained to a very small area.

As for the *Vp/Vs* ratio we believe that also the obtained crustal velocity model is applicable for larger areas in eastern Iran.

For some events in this aftershock database focal mechanisms could be computed. The focal mechanisms show preferences for strike slip mechanisms in accordance with the main rupture. However, the components of both thrust and normal faulting indicate a complex deformation pattern in the larger volume around the main fault.

Finally, three of the aftershocks have been

investigated with respect to its usefulness for calibrating travel times over large regions (defining the hypocenters with high precision). The three events that were recorded on a large number of regional stations could be located with the temporal networks and the new velocity model to Ground Truth locations better than 5 to 10km. The relocation results of three selected aftershocks with new crustal model regarded as the best parameters of these events in contrast of considerable azimuthal gaps.

While we regard the above as useful and important results that contribute both in seismicity location related problems of the region and to the tectonic understanding, the database also highlights some problems that an aftershock campaign may encounter. Firstly, it was realized that the distribution of instruments is severely dependent on accessibility and security for the instruments. As for the Ghaen-Birjand region this caused an uneven distribution of the temporal network stations to the west of the main rupture zone. Secondly, it became clear how vulnerable such temporal networks are to technical problems. Even with the significant station redundancy in the two networks the data acquisition suffered severely under technical problems, and this entailed that many events were recorded on few stations.

Acknowledgments

References

1. Ambraseys, N.N. and Melville, C. (1982). "A History of Persian Earthquakes", Cambridge University Press, Cambridge.

2. Asudeh, I. (1982). "Seismic Structure of Iran from Surface and Body Wave Data", *Geophys. J. R. Astr. Soc.*, **71**, 715-730.

3. Bahavar, M. (1995). "A Crustal Structure Model for Eastern Iran Using Rayleigh Wave Phase Velocity Dispersion", IIEES Internal Report.

4. Berberian, M. (1982). "Aftershock Tectonics of the 1978 Tabas-e-Golshan (Iran) Earthquake Sequence: A Documented Active `Thin and Thick-skinned Tectonic' Case.", *Geophys. J. Roy. Astr. Soc.*, **68**, 499-530.

5. Berberian, M., Jackson, J.A., Qorashi, M., Khatib, M.M., Preistley, K., Talebian, M., and Ghafuri-Ashtiani, M. (1999). "The 1997 May 10 Zirkuh (Qa'enat) Earthquake (Mw 7.2): Faulting Along the Sistan Suture Zone of Eastern Iran", *Geophys. J. Int.*, **136**(3), 671-649.

6. Berberian, M. and Yeats, R.S. (1999). "Patterns of Historical Earthquake Rupture in the Iranian Plateau", B.S.S.A., **89**(1), 120-139.

7. Farahbod, A.M., Yamini-Fard, F., and Taleb Hessami-Azar, Kh. (1998). "A Review of Ardekul Earthquake and its Aftershocks", IIEES Publication, No. 77-98-4.

8. Jackson, J. and Mckenzie, D. (1984). "Active Tectonics of the Alpine-Himalayan Belt between Western Turkey and Pakistan", *Geophys. J. Roy. Astr. Soc.*, **77**, 185-264.

9. Kissling, E. (1995). "VELEST User's Guide, Institute of Geophysics, ETH Zurich, 25 pp.

10. Kissling, E. (1988). "Geotomography with Local Earthquake Data", *Rev. of Geophysics*, **26**, 659-698.

11. Kissling, E., Ellsworth, W.L., Eberhart-Phillips, D., and Kradolfer, U. (1994). "Initial Reference Models in Local Earthquake Tomography", *J. Geophys. Res.*, **99**, 19635-19646.

12. Moazami-Goudarzi, K. and Sadeghzadeh, N. (1972). "Un Modele a Deux Couches Pour La Croute Terrestre Dans Le Sud De L' Iran", *J. of the Earth and Space Physics*, **1**(1).

13. Naderzadeh, A. and Khademi, M.H. (1997). "A Preliminary Report on the Ardekul, Iran Earthquake of 10 May 1997", Centre for Earthquake Studies of Tehran (CEST).

14. Nikzad, K., Alinaghi, A., Azadi, A., and Farahbod, A.M. (1997). "A Preliminary Report on the Ardekul (Ghaen-Birjand) Earthquake of May 10, 1997", IIEES Publication, No. 76-67-10.

15. Raeesi, M. (1998). "Analysis of 1997 May 10, Zirkuh (Ghaen-Birjand) Earthquake", M.Sc. Thesis, Institute of Geophysics of Tehran University.

16. Sweeney, J.J. and Walter, W.R. (1998). "Preliminary Definition of Geophysical Regions for the Middle East and North Africa", Lawrence Livermore National Laboratories, UCRL-ID-132899.

17. Tirrul, R., Bell, I.R., Griffis, R.J., and Camp, V.E. (1983). "The Sistan Structure Zone of Eastern Iran", *Geological Society of America Bulletin*, **94**, 134-150.

18. West, M. (1999). "The Ardekul Iran Earthquake of May 10, 1997", Website: www.ldeo.columbia.edu/~mwest/.